Macromolecules 1987, 20, 689–693

Morphological Study of Supported Chromium Polymerization Catalysts. 1. Activation

E. L. Weist, Ahmed H. Ali,[†] and W. C. Conner*

Department of Chemical Engineering, University of Massachusetts, Amherst, Massachusetts 01003. *Received August 11, 1986*

ABSTRACT: The high-temperature treatments in the activation of Phillips polymerization catalysts cause dramatic changes in the morphology of the silica support. The void structure of three commercial catalysts supplied by Phillips with pore volumes of 1.1, 1.7, and 2.3 cm^3/g were studied by using mercury porosimetry. It was found that the higher pore volume systems were similar in many ways but were different from the 1.1 cm^3/g catalyst after the various activation treatments. The similarities included similar pore volume inside pores with diameter larger than 20 nm, bimodal pore-size distribution, and almost the same ethylene polymerization activity.

Introduction

In the polymerization of ethylene using supported chromium catalysts, the structure of the support may influence both the polymerization activity and the resulting polymer. A support that has a high pore volume and fractures easily generally exhibits greater activity. Chromium deposited on a support with large pores produces a lower molecular weight polymer.[1] Since these discoveries, there has been a need to examine more closely how the catalyst morphology affects the polymerization process. In a recent review article, Karol stated, "Catalyst characterization studies and use of model reactions appear necessary in studies relating catalyst structure to polymer molecular weight distribution".[2]

Earlier studies have shown that the total pore volume, the average pore size, and the surface area of the catalyst have significant influence on polymerization activity. Carrick et al. impregnated a variety of silica supports with average pore diameters ranging from 2.2 to 20 nm with bis(triphenylsilyl) chromate.[3] The results indicate that the average pore diameter of the support should be at least 6.7 nm for adequate polymerization activity. McDaniel found that the activity of 2% titanium on a silica support of 1.6 cm^3/g pore volume was an order of magnitude higher than that of 2% titanium on a silica support of 0.43 cm^3/g pore volume.[1] However, the activity of 2% titanium on a 3.2 cm^3/g pore volume support was only slightly higher than that for the 1.6 cm^3/g pore volume support. Similar results were found for chromium–silica catalysts. Munoz-Escalona et al. also found greater activity when titanium was deposited on a support with a pore volume of 1.6 cm^3/g compared to 0.9 cm^3/g.[4]

Little research has been conducted to understand how the void structure of the support influences the polymerization. McDaniel studied the fracturing of supported chromium and titanium catalysts by removing the polymer from the fragmented catalyst after reaction.[1] The catalysts were characterized by nitrogen sorption before and after polymerization. The polymerization did not change the surface area, but increased the pore volume in the macropores (defined by McDaniel as >60-nm diameter). From this observation he concluded that fracturing occurred along pores greater than 60 nm in diameter, and, therefore, a greater amount of macropores results in a higher polymerization activity due to the fracture of the support. However, 60 nm is beyond the range of pore sizes measurable by nitrogen sorption. McDaniel has recently published a study using mercury porosimetry to characterize the pore structure of the catalysts.[5] In this work chromium was deposited on a series of porous silica supports in which the pore volume and pore-size distribution were varied by using different methods of preparation. As before, the polymerization activity increased with increasing total pore volume. There also seemed to be a correlation between the activity and the amount of pore volume in pores with diameters in the range 10–100 nm. Characterization by porosimetry before and after polymerization showed that there was an increase in the pore volume in pores greater than 30 nm, and thus fracturing occurred along pores greater tham 30 nm in diameter.

In comparison to nitrogen adsorption, mercury porosimetry is suited to the study of pore sizes in the macropore region. Indeed, it is applicable from 4 to 10^4 nm in pore diameter. Porosimetry has not been used extensively in the study of polymerization catalysts. The studies referred to above have involved comparison of the morphology of the activated catalysts to the activity. In light of the severe conditions required for catalyst pretreatment (often in excess of 850 °C), it is necessary to quantify the morphological changes that occur due to both pretreatment and activation processes. By observing the changes in the porosimetry data of the catalyst after the activation process and, subsequently, after the initial stages of polymerization, we may be able to infer what is happening to the support during these processes. From this analysis we may gain insight into the changes in the catalyst void structure as it relates to olefin polymerization.

Experimental Section

Catalyst. The Phillips Petroleum Co. has supplied chromium oxide on silica catalysts similar to their commercial catalysts. These catalysts are all approximately 1% chromium deposited on three different silica supports of nominal pore volumes: 1.1–1.2, 1.6–1.7, and 2.2–2.3 cm^3/g. The first two supports are Davison silica gels, while the last is a silica gel developed by Phillips.

Activation Procedure. In a vertical furnace, the catalysts were first calcined in dry oxygen at elevated temperatures (500–870 °C) and then reduced in carbon monoxide at 400 °C if desired. The temperature was raised from room temperature at a rate of 400 °C/h under flowing oxygen until the desired calcination temperature was reached. The temperature was held constant for 5 h and then cooled to room temperature. The calcined catalyst is now active for ethylene polymerization; however, after exposure to ethylene, there is an induction period ranging from a few minutes to an hour before polymerization begins.[6]

This induction period can be eliminated if the chromium is prereduced with carbon monoxide.[6] If the samples were to be treated with carbon monoxide, the calcined catalyst was first cooled to 400 °C under flowing oxygen. The gas flow was then switched from oxygen to nitrogen and then to carbon monoxide, and the temperature was maintained at 400 °C for 3 h. Because carbon monoxide is believed to be a reversible poison,[7] it is presumed to be displaced from the catalyst surface by flowing nitrogen after about 10 min at 400 °C. The catalyst was then

---

* Author to whom correspondence should be addressed.

[†] Present address: Mobil Research and Development, Edison, NJ.

0024-9297/87/2220-0689$01.50/0

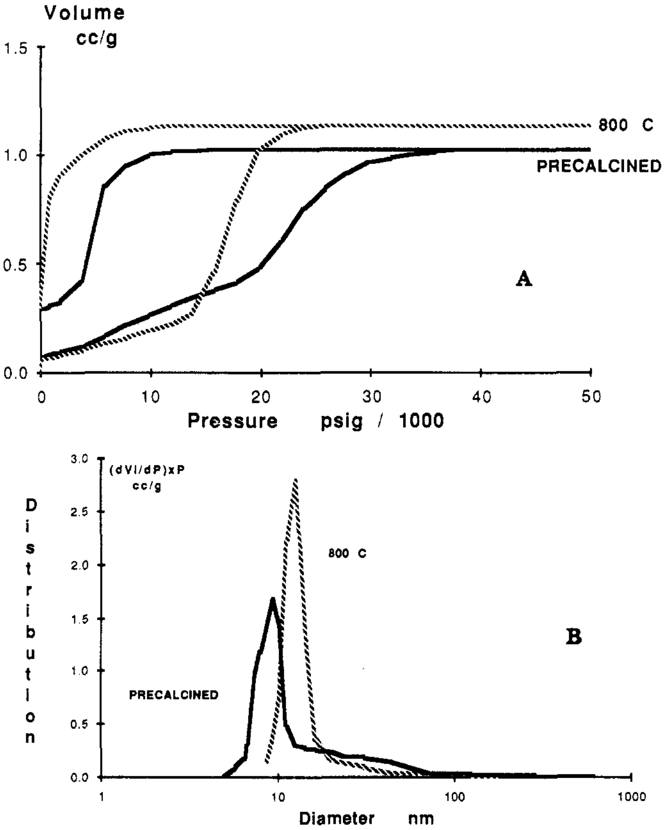

Figure 1. (A) Effect of calcination temperature on the porosimetry plot of the 1.1 cm^3/g catalyst. (B) Effect of calcination temperature on the constriction-size distribution of the 1.1 cm^3/g catalyst.

cooled to room temperature under nitrogen. The blue catalyst that resulted was active for ethylene polymerization.

Porosimetry. Mercury porosimetry characterization was performed by using a Quantachrome scanning mercury porosimeter capable of pressures up to 60 000 psig. The pressure, P, may be related to the pore diameter, d, by using the Washburn equation with a contact angle, θ, of 140°, and a surface tension, γ, of 480 dyn/cm, i.e., $Pd = 4\gamma \cos \theta$.[8] Thus, this porosimeter allows us to characterize void dimensions from 4 to 10^4 nm. The sample cells were filled with mercury by using a Quantachrome Autoscan 500 porosimeter after outgassing to less than 0.1 Torr.

The porosimetry studies were performed on the catalysts after exposure to the atmosphere, and the results are based on the sample weight. Thus, the fresh unactivated catalysts contain adsorbed surface-water molecules that decrease the amount of pore volume within the pellet and increase the pellet density. The combination of these two effects decreases the specific pore volume; however, the adsorbed water molecules do not affect the pore-size distribution. The amount of adsorbed volatiles was determined to be approximately 8–10% by weight. When carbon monoxide reduced catalysts were studied, the samples were transferred to the porosimetry cell in a glovebox under a nitrogen or argon atmosphere.

The conventional utilization of mercury porosimetry data is to interpret the intrusion curve as reflecting the pore-size distribution (PSD). This interpretation is based on a model of the void structure as a series of nonintersecting cylindrical pores. This is rather unrealistic. Our recent studies suggest that the intrusion curve measures not the PSD, but the sizes of the constrictions (throats) that connect larger openings (pores) within the sample.[9] This model views the void structure as an interconnected network of voids linked by constrictions. The extrusion process measures the sized of the openings within the network.

In this paper we are going to refer to the constrictions and give their diameters in nanometers (nm), as determined by the intrusion curve. The size distribution of these constrictions is somewhat similar to the classical interpretation of the intrusion curve which was thought to determine the pore sizes. We will only examine the size distribution of the constrictions as given by the intrusion curve. Detailed analyses that use the extrusion as well as the intrusion curve will appear elsewhere.[10] In this paper we use macroporosity when referring to pores greater than 20 nm in diameter, microporosity for pores smaller than 4 nm in diameter, and mesoporosity for the region between 4 and 20 nm.

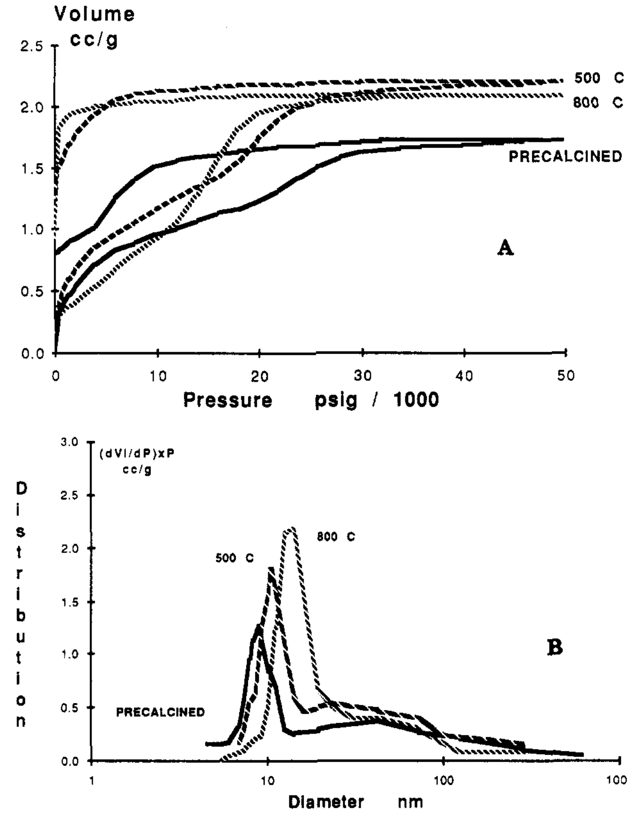

Figure 2. (A) Effect of calcination temperature on the porosimetry plot of the 1.7 cm^3/g catalyst. (B) Effect of calcination temperature on the constriction-size distribution of the 1.7 cm^3/g catalyst.

Surface Area. Surface area measurements were made by using nitrogen sorption in a volumetric apparatus. This apparatus was used to measure adsorption at five pressures from 40 to 200 Torr at liquid nitrogen temperature. The surface area was calculated by using the BET equation.

Results

Calcination Temperature. Figure 1A shows the mercury porosimetry intrusion and extrusion curves for the 1.1 cm^3/g catalyst before and after calcination at 800 °C. The specific intruded pore volume is plotted against the applied pressure. The corresponding volume distribution of the constrictions is shown in Figure 1B. This plot is generated by taking the derivative of the intrusion curve with respect to pressure. To obtain units in volume per weight (cm^3/g), the derivative is multiplied by the applied pressure. After calcination, the pore volume connected via constrictions greater than 20 nm has decreased slightly, and the regions of intrusion and extrusion have shifted to larger void dimensions. In addition to this shift, the slope of the intrusion curve is steeper; thus, the distribution curve becomes narrower as the maximum of the peak shifts from 9.5 to 12.5 nm. There is a slight increase in the total pore volume due to the removal of adsorbed water.

Figure 2A shows the mercury intrusion and extrusion curves for the 1.7 cm^3/g catalyst before and after calcination at 500 and 800 °C. Figure 2B shows the volume distribution of the constrictions in the sample that lead into the voids. The mesopore void structure for this

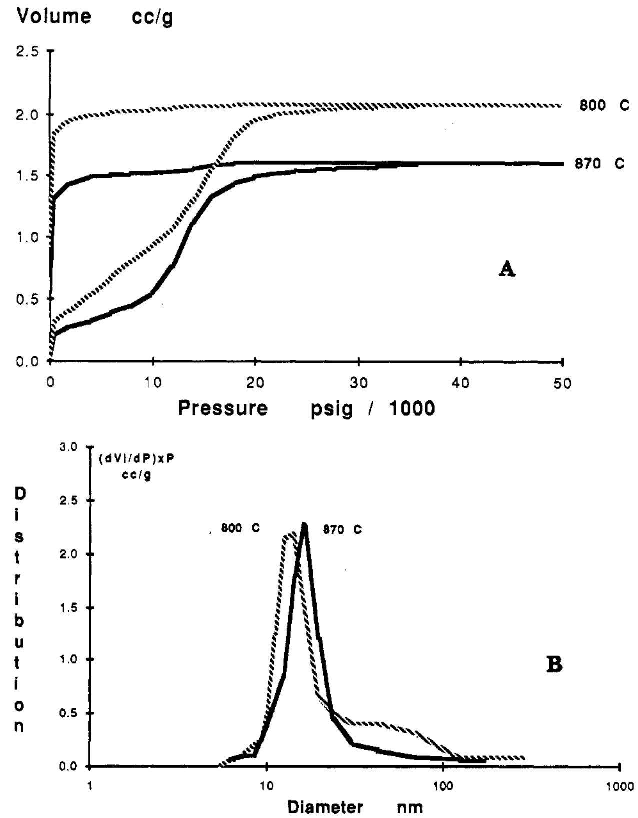

Figure 3. (A) Effect of calcination at 870 °C on the porosimetry plot of the 1.7 cm^3/g catalyst. (B) Effect of calcination at 870 °C on the constriction-size distribution of the 1.7 cm^3/g catalyst.

catalyst is very similar to that of the 1.1 cm^3/g catalyst; however, this catalyst has a significant amount of pore volume connected via constrictions greater than 20 nm in diameter. The removal of the adsorbed water molecules by calcination at 500 °C increases the total pore volume measured by porosimetry. The pore volume in the macropore region increases and then decreases as the calcination temperature is raised to 800 °C. As in the 1.1 cm^3/g catalyst, the pore-size distribution in the mesopore region narrows and shifts to larger sizes (from 9 to 13.5 nm) as the calcination temperature increases.

Figure 3A shows the porosimetry data after this catalyst has been calcined at 800 and 870 °C. At 870 °C, the calcination temperature is near the sintering point of the silica. There is a large decrease in the total pore volume, especially in the macropore region. A further shift to larger sizes and a narrowing of the distribution in the small mesopore region is seen in Figure 3B.

Figure 4A shows the porosimetry plots for the 2.3 cm^3/g catalyst after calcination at 500 and 800 °C. Figure 4B shows the distribution of the constrictions. Before calcination, this catalyst has almost all its pore volume connected via constrictions greater than 10 nm in diameter. After calcination at 500 °C, small constrictions of about 5 nm develop. As in the other catalysts, this region shifts to larger void sizes as the distribution becomes narrower with higher calcination temperatures as shown in Figure 4B. Also, the pore volume in the larger pores decreases after calcination at 800 °C.

Reduction at 400 °C. Figure 5 shows the effect of a 3-h reduction with carbon monoxide at 400 °C on the morphology of the 2.3 cm^3/g catalyst. There is a slight decrease in the pore volume for all regions of intrusion and extrusion. The other catalyst samples also displayed a similar loss of pore volume after treatment with carbon monoxide at 400 °C.

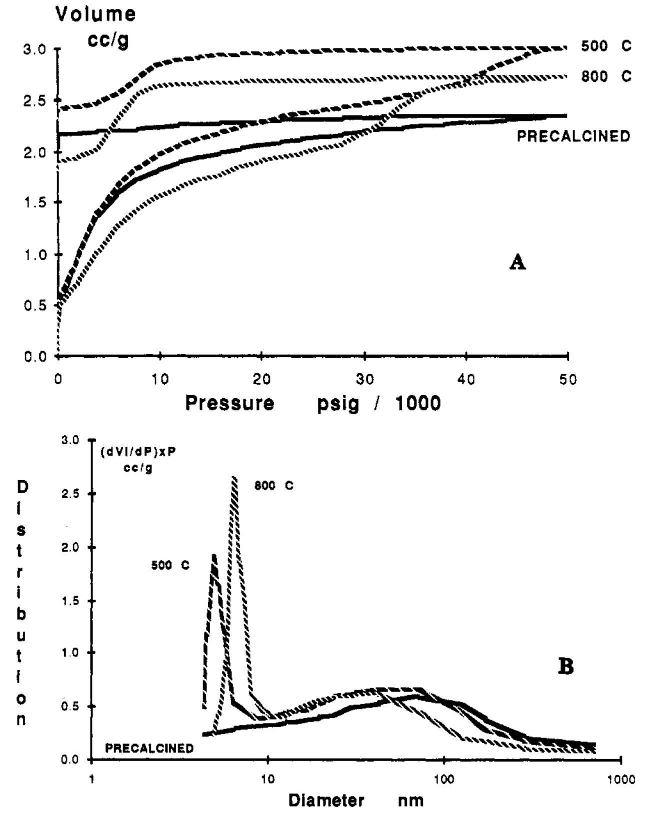

Figure 4. (A) Effect of calcination temperature on the porosimetry plot of the 2.3 cm^3/g catalyst. (B) Effect of calcination temperature on the constriction-size distribution of the 2.3 cm^3/g catalyst.

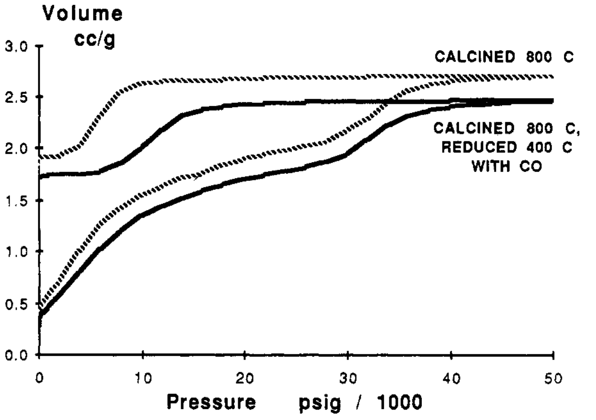

Figure 5. Effect of carbon monoxide reduction at 400 °C on the 2.3 cm^3/g catalyst.

Analysis

Calcination Effects. It is clear from the plots shown that calcination has changed the internal void structure of these catalysts as measured by porosimetry. However, these changes were not the same for each sample of different pore volume. The shifting of the size distribution and the decreasing macropore pore volume are seen for all samples. These changes can be better understood if we look at the influence of calcination on a high-surface-area silica of known morphology. To this end, we studied a sample of compacted microspheres (Degussa Aerosil A-380) after calcination at various temperatures.

Aerosils are nonporous, monodisperse, silica particles. To create a void structure, these 7-nm spheres were compressed at 10 000 psi. Figure 6 shows the porosimetry of the compressed sample before and after calcination at 500 and 800 °C. As the calcination temperature is increased,

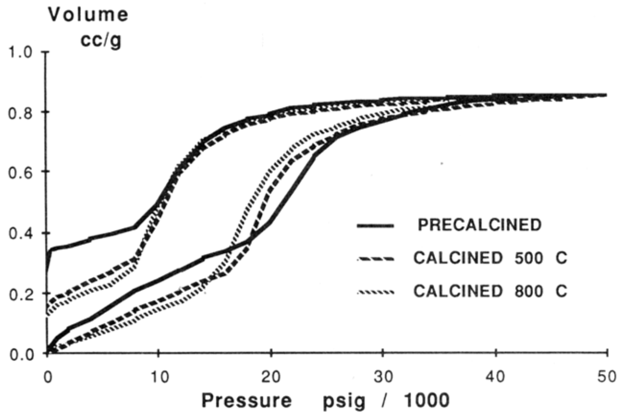

Figure 6. Effect of calcination temperature on compacted Aerosil 380.

Table I
Effect of Catalyst Pretreatment on Surface Area

	catalyst surface area, m^2/g		
catalyst	1.1 PV^a	1.7 PV^a	2.3 PV^a
precalcined	280	285	470
calcined (800 °C)	230	221	420
activated (800/400 °C)	280	231	430

^{a} PV, pore volume.

the pore volume inside constrictions larger than 15 nm is seen to decrease, and the pore volume inside constrictions between 4 and 15 nm increases. There is also a concomitant shift in the constriction size distribution toward larger sizes.

A parallel decrease in surface area was also noted. The surface area decreased from 380 m^2/g in the precalcined sample to 334 m^2/g after calcination at 800 °C. This is attributed to sintering of the smaller constrictions. This is supported by the shift in the size distribution of the constrictions toward larger sizes. The detection of the microconstrictions, those less than 4 nm in diameter, is not possible with porosimetry.

With this background, let us examine the changes in the Phillips catalysts after calcination and after activation. After calcination at 800 °C, the 1.7 and 2.3 cm^3/g catalysts had significant losses in macroporosity, as measured by intrusion, in comparison with the 1.1 cm^3/g catalyst. This trend was also observed in the Aerosil A-380. On the other hand, the 1.1 cm^3/g catalyst did not have much macroporosity before calcination.

After calcination at 500 °C, there is an increase in the pore volume, especially in the macropores, in the polymerization catalysts. This occurs with the simultaneous removal of surface-water molecules and condensation of hydroxyl groups. Thus, there is a slight increase in the size of the pores coupled with a decrease in the catalyst pellet density, resulting in an increase of the specific pore volume.

Both the compacted Aerosils and the polymerization catalysts exhibited an increase in the average constriction size and a narrowing of the distribution in the mesopore region due to the collapse or coalescence of small pores to form larger ones. The shifting of the void dimensions (pores and constrictions) toward larger sizes is accompanied by a drop in the surface area in the polymerization catalysts as well as in the compacted Aerosils. Table I shows that the surface area of the catalysts decreases about 50–60 m^2/g after calcination at 800 °C.

Calcination not only dehydrates the surface of the Aerosil but also modifies the void structure. These modifications in the constrictions appear across the pore size spectrum. The formation of large constrictions from the collapse or coalescence of the smaller constrictions is indicated by the loss of surface area and the shift in the size distribution. The losses in the macroporous pore volume are also indicative of the void-structure modifications in the sample.

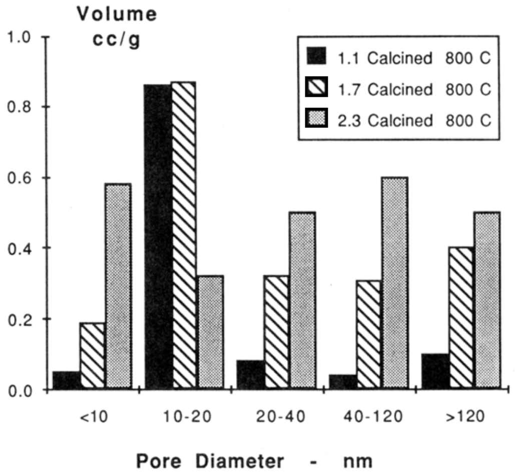

Figure 7. Comparison of the volume distribution of the three polymerization catalysts after calcination at 800 °C.

Reduction Effects. From Table I it can be seen that the surface area of the three catalysts increased after reduction in carbon monoxide at 400 °C, particularly for the 1.1 cm^3/g catalyst. These increases were 50, 15, and 10 m^2/g for the 1.1, 1.7, and 2.3 cm^3/g catalysts, respectively. While the latter two figures are within the error margins of the BET method (±10%), the first figure for the 1.1 cm^3/g pore volume catalyst is significant.

The accurate determination of the surface area is important in the estimation of the catalyst active site density. Since surface area is primarily determined by microvoids, a change in these was somehow induced by the carbon monoxide in the case of the 1.1 cm^3/g system. It was shown in Figure 5 that reduction did not alter the pore-size distribution of the activated sample in comparison with the calcined sample. This indicates that constrictions smaller than 4 nm have been made accessible to nitrogen after activation. As noted before, voids smaller than 4 nm cannot be measured with our porosimeter. Since the chromium loading is about 1%, the reduction of chromium should not roughen the surface and increase the surface area unless actual cracks or fissures were formed or uncovered in the process.

Similarities and Differences in Void Structure. A comparison of the void structure of the three catalysts will be presented. In the second part of this series the differences in the void structure of the active catalysts will be related to the differences in activity for ethylene polymerization.[11] We believe this perspective is crucial to our understanding of the effects of catalyst fragmentation during ethylene polymerization.

It is clear that the two higher pore volume catalysts are similar; however, they are different from the 1.1 cm^3/g system. In Figure 7 the void volume accessed by the indicated constriction size ranges, on the abscissa, is shown after calcination of the catalysts at 800 °C. The 1.7 and 2.3 cm^3/g catalysts have a significant amount of pore volume connected by constrictions greater than 20 nm. On the other hand, the 1.1 cm^3/g catalyst contains very few pores in this region. In the case of the 1.1 and 1.7 cm^3/g catalysts, the volume distributions are roughly the same for voids less than 20 nm.

Table II
Polymerization Activity as a Function of the Silica Support

	catalyst pore volume		
	1.1 cm^3/g	1.7 cm^3/g	2.3 cm^3/g
activity, g of PE/(g of catalyst·atm·h)	3.9	20.5	26

In short, while the 1.7 and 2.3 cm^3/g catalysts are similar in macroporosity, the 1.1 and 1.7 cm^3/g systems resemble each other primarily in mesoporosity. The void-size distributions for the catalysts of the 1.7 and 2.3 cm^3/g systems are bimodal after activation. The 1.1 cm^3/g is clearly unimodal.

In the case of the compacted Aerosils, it was seen that calcination shifted the size distribution of the constrictions. Calcination also decreased the surface area as well as the volume in the macrovoids. These changes were due to either the collapse or the coalescence of the voids in both macro- and mesopore regions. The three Phillips catalysts also were affected similarly by the heat treatment. This suggests that these phenomena may be general to silica gels. It is even more important to realize that these commercial and lab gels may have a structure that is equivalent to an agglomeration of subparticles. Therefore, the changes in the void structures, which were initially formed by the agglomeration, will also explain the surface-area losses as well as the shifts in the size distributions of the voids.

Activity. For similarly activated catalysts having equivalent metal loading, the polymerization activity has been shown to be dependent on the catalyst morphology.[1,5] The dependence of activity on morphology was tested by using low-pressure (up to 1 atm in ethylene) gas-phase polymerization in a modified Cahn electrobalance. The catalyst was calcined in situ in flowing oxygen at 800 °C. After the catalyst was cooled to room temperature, Phillips' polymerization grade ethylene was supplied intermittently to keep the pressure at approximately 500 Torr. The activities given in Table II were found by calculating the derivative of the weight gain vs. time curve. The maximum in this curve corresponds to a maximum instantaneous activity, and it is this value which was chosen as a measure of the activity.

Table II shows some of the experimental rate constants for the three active catalysts. These catalysts were all calcined at 800 °C for 5 h. The activity was found to increase from 3.9 g of PE/((g of catalyst)·atm·h) at 110 °C with the 1.1 cm^3/g catalyst to 20.5 g of PE/((g of catalyst)·atm·h) when the 1.7 cm^3/g catalyst was utilized. The activity of the 2.3 cm^3/g catalyst was 26 g of PE/((g of catalyst)·atm·h). It is seen that an order of magnitude increase in activity results when the higher pore volume systems (1.7 and 2.3 cm^3/g) are used in comparison with the 1.1 cm^3/g catalyst. This points to the preferential use of higher pore volume systems on the basis of their activity.

It is not only necessary to have high-pore-volume catalysts (>1.7 cm^3/g) but the catalysts should have large macroporosity, i.e., substantial pore volume inside void sizes larger than 20 nm. These are thought to strongly influence the polymerization activity. It is also evident that additional pore volume, larger than that of the 1.7 cm^3/g system, does not result in any substantial increase in polymerization rate. Any additional increase in pore volume may, however, affect the quality of the porduct. There have been studies that indicate that the higher pore volume systems produce resins with higher melt indices.[1,3,5] Macroporosity not only leads to higher polymerization activity but also affects the extent of fragmentation of these catalysts during polymerization. Macroporous supports are thought to be more susceptible to fragmentation.[1]

Conclusions

It was shown that, depending on the initial morphology of the catalyst, significant changes take place in the catalyst void structure after calcination and upon activation. Calcination affected both the pore-size distribution and the catalyst surface area, while reduction in carbon monoxide primarily changed the surface area. The accurate measurement of microporosity is beyond the limit of porosimetry. All the above changes need to be quantified, understood, and taken into account in comparing catalysts. These studies can also be used as a tool in understanding activity and product quality differences produced by different catalysts. Activity differences between the three Phillips catalysts were related to their differences and similarities in terms of macroporosity. The two higher pore volume systems were shown to be similar in their morphology as well as in their activity in comparison with the 1.1 cm^3/g catalyst.

In modeling polymerization reactors that use supported coordination catalysts, increasing attention is being paid to the effects of fragmentation. More realistic models have recently included fragmentation dynamics.[11] In order to better model these processes, it is crucial to have a clear picture of the void structure of the active catalyst. These models should be based on the activated catalyst rather than on the precalcined or even the calcined sample. We have shown in this study that there are significant variations after each treatment.

Acknowledgment. We thank Union Carbide Corp. for supporting this as well as the ongoing work in this area. The National Science Foundation, under grant NSF CPE 81-21800, also supported this project. Phillips Petroleum is graciously acknowledged for supplying us with catalysts. John Neal is thanked for doing the sintering studies on the compacted Aerosils. Finally, we thank Juan R. Gonzalez-Velasco for doing some of the surface-area measurements.

Registry No. PE, 9002-88-4; chromium oxide, 11118-57-3.

References and Notes

(1) McDaniel, M. P. *J. Polym, Sci., Polym. Chem. Ed.* **1981**, *19*, 1967.
(2) Karol, F. J. *Catal. Rev.-Sci. Eng.* **1984**, *26*, 557.
(3) Carrick, W. L.; Turbett, R. J.; Karol, F. J.; Karapinka, G. L.; Fox, A. S.; Johnson, R. N. *J. Polym. Sci., Polym. Chem. Ed.* **1972**, *10*, 2609.
(4) Munoz-Escalona, A.; Hernandez, J. G.; Gallardo, J. A. *J. Appl. Polym. Sci.* **1984**, *29*, 1187.
(5) McDaniel, M. P. *Adv. Catal.* **1985**, *33*, 47.
(6) Merryfield, R.; McDaniel, M.; Parks, G. *J. Catal.* **1982**, *77*, 348.
(7) Hogan, J. P. *J. Polym. Sci., Polym. Chem. Ed.* **1970**, *8*, 2637.
(8) Gregg, S. J.; Singh, K. S. W. *Adsorption, Surface Area, and Porosity*; Academic: London, 1982; p 175.
(9) Conner, W. C.; Lane A. M. *J. Catal.* **1984**, *89*, 217.
(10) Conner, W. C.; Weist, E. L.; Ali, A. H.; Laurence, R. L. Presented at the International Symposium on Transition Metal Catalyzed Polymerization; Akron, OH; June 16-20, 1986.
(11) Ali, A. H.; Weist, E. L.; Conner, W. C., to be submitted to *Macromolecules*.
(12) Laurence, R. L.; Chiovetta, M. In *Polymer Reaction Engineering, Influence of Reaction Engineering on Polymer Properties*; Reichert, K. H., Geiseler, W., Eds.; Hanser: Munich, 1983; p 73.